J. Phys. F: Met. Phys., 12(1982)1861–8. Printed in Great Britain

The structure and properties of some $Rh_{0.92-x}B_xSi_{0.08}$ metallic glasses

Arthur Williams, Madhav Mehra and William L Johnson
W M Keck Laboratory of Engineering Materials, California Institute of Technology, Pasadena, California 91125, USA

Received 19 January 1982, in final form 5 March 1982

Abstract. Rhodium-based metallic glasses have been produced with over 40 at% metalloids (Si and B). X-ray diffraction studies are presented here on $Rh_{0.92-x}B_xSi_{0.08}$ metallic glasses, with $x = 0.22$, 0.27 and 0.32, as well as mechanical, electrical and thermal analysis data. The structural studies suggest that this system undergoes a considerable change in short-range order with increasing boron concentration.

1. Introduction

It is well known that a large number of transition-metal–metalloid alloys can be quenched rapidly from the melt into an amorphous phase. The range of composition over which these alloys are ready glass formers is always more or less centred about a deep eutectic in the phase diagram and in most cases lies between 17 and 25 at% metalloid. Recently, however, Ni–B and Co–B metallic glasses have been reported with boron concentrations as high as 40 at% (Inoue *et al* 1979, Chadha *et al* 1981). The commonly held picture of the structure of such metallic glasses as dense random packings with metalloid atoms occupying the large polyhedral holes is clearly not acceptable for alloys with such high metalloid concentrations. We report here on the discovery of some rhodium-based ternary metallic glasses with about 30–40 at% metalloids which appear from x-ray studies to exhibit a considerable change in short-range order with increasing metalloid concentration. These alloys have been found to be extremely resistant to chemical attack, are very ductile and not particularly hard despite the high metalloid content. X-ray, thermal analysis and high-temperature resistivity measurements all confirm the fact that these alloys are truly amorphous and not microcrystalline.

2. Experimental procedure

All alloys were prepared by RF induction melting on a water-cooled silver boat. Samples were prepared by rapid quenching from the melt in a helium atmosphere using the piston and anvil technique (Pietrokowsky 1963), producing foils typically 35 μm thick and 1 cm in diameter. Samples were checked for crystallinity using a Norelco scanning diffractometer and Cu Kα radiation. The more accurate x-ray

0305-4608/82/091861 + 08 $01.50

MP(F) 12 9—A

diffraction studies were performed on a GE XRD-5 diffractometer with Mo Kα radiation and a focusing LiF monochromator in the diffracted beam. Data were corrected for background, polarisation, absorption and Compton scattering and were normalised using the well known high-angle method (Cargill 1975). Densities were measured using the hydrostatic weighing technique with toluene as the working fluid. Several foils were measured for each composition and the results averaged together to obtain the representative value.

Hardness measurements were performed on a Leitz microhardness tester using a diamond pyramid. A mass of typically 50–100 g was used for the measurements.

The low-temperature resistivity measurements were performed using the van der Pauw (1958) technique. The sample was cut into a circular shape and four pressure contacts placed on it. To monitor the temperature a chromel–(Au–0.07 at% Fe) thermocouple was used. Typically, currents of 10.0 mA were employed.

For the high-temperature resistivity, platinum contacts were spot welded onto a strip of the sample and the latter was continuously heated in a furnace. The heating rate quoted was the average heating rate and is not representative of the heating rate at the crystallisation temperature (T_x). The temperature was monitored using a platinum–(Pt–10 at% Rh) thermocouple. In all the resistivity studies the effect of thermal voltages was eliminated by reversing the direction of the current for each measurement.

The differential thermal analysis (DTA) study was carried out using a Dupont 1090 'differential thermal analyser'. The heating rates are quoted. The curves shown have been normalised with respect to the baseline of the two crucibles alone.

3. Results

The ternary alloy $Rh_{0.92-x}B_xSi_{0.08}$ was found to be amorphous when rapidly quenched from the melt in the composition range $0.20 \lesssim x \lesssim 0.34$. For $x < 0.20$, primary crystallisation of FCC rhodium occurs, while for $Rh_{56}B_{36}Si_8$ for example, the amorphous phase was found to coexist with an unidentified crystalline phase. Attempts to produce amorphous foils without silicon or to substitute Ge for Si failed, although $Rh_{56}Ti_{10}B_{34}$ was also found to be a ready glass former. All of the rhodium-based glassy foils produced were very ductile and extremely resistant to chemical attack. In fact, all efforts to electrochemically etch samples thin enough for TEM study were fruitless. X-ray diffraction studies were performed, however, which showed an exceptionally broad primary maximum and large secondary maximum especially at large boron concentrations. Figure 1 shows the reduced interference functions, $i(K) = K(I(K) - 1)$, for three $Rh_{0.92-x}B_xSi_{0.08}$ metallic glasses at $x = 0.22$, 0.27 and 0.32, in which the trends of increasingly broad primary maxima are clearly seen. In $Rh_{60}Si_8B_{32}$ the unusual fact that the second peak is larger than the first, together with the large number of well defined peaks, suggested that the material might be some oriented microcrystalline phase. This was shown not to be the case, however, by performing experiments in both reflection and transmission geometries with identical results, also shown in figure 1.

The reduced radial distribution functions, $G(r)$, obtained from

$$G(r) = \frac{2}{\pi}\int_0^{K_{max}} K(I(K) - 1)\sin Kr \exp(-\alpha K^2)\, dK$$

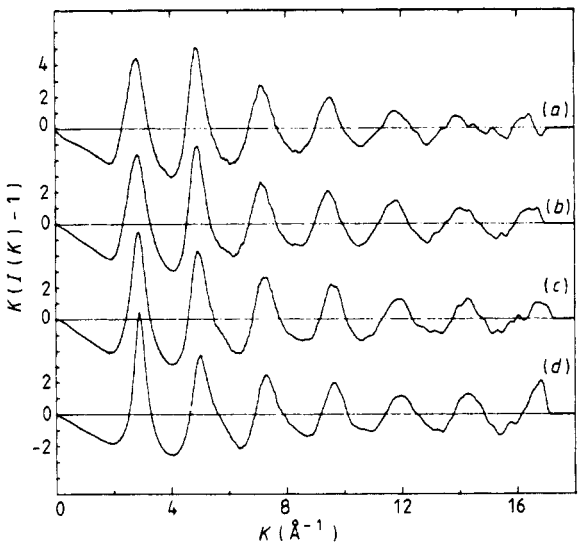

Figure 1. The reduced interference functions $i(K) = K(I(K) - 1)$, obtained from x-ray diffraction data for three rhodium-based metallic glasses. Data for $Rh_{60}Si_8B_{32}$ using both a reflection and a transmission geometry are included. (*a*) $Rh_{60}B_{32}Si_8$ (transmission); (*b*) $Rh_{60}B_{32}Si_8$ (reflection); (*c*) $Rh_{65}B_{27}Si_8$; (*d*) $Rh_{70}B_{22}Si_8$.

are shown in figure 2. For this case the well known convergence factor $\exp(-\alpha K^2)$ (Cargill 1975) was used with $\alpha = 0.004$, to help alleviate the ripples introduced from termination of the integral at $K_{max} \simeq 17.7$ Å^{-1}, which is the maximum wavevector accessible with Mo Kα radiation.

The positions of the first four maxima in the three $G(r)$ shown in figure 2 are listed in table 1, along with atomic densities and coordination numbers. R_1, which is just the

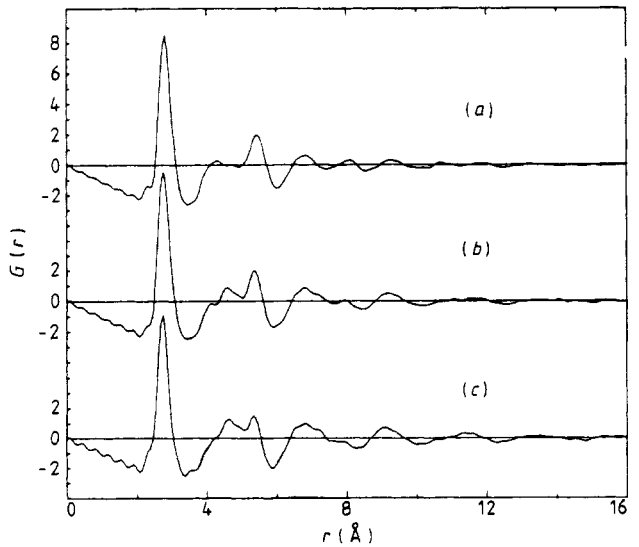

Figure 2. The reduced radial distribution functions $G(r) = 4\pi r(\rho(r) - \rho_0)$, obtained from the x-ray interference functions for three rhodium-based metallic glasses. (*a*) $Rh_{60}B_{32}Si_8$; (*b*) $Rh_{65}B_{27}Si_8$; (*c*) $Rh_{70}B_{22}Si_8$.

average nearest-neighbour distance, increases rapidly with increasing boron concentration and is, in all cases, larger than the FCC metallic rhodium interatomic distance of 2.68 Å. Even more interesting is the disappearance of the peak near $1.67(R_3/R_1)$ and subsequent growth of a distinct maximum near $1.5(R_2/R_1)$ with increasing boron content. A split second maximum in the $G(r)$, with peaks near 1.67 and 1.95 as displayed by $Rh_{70}B_{22}Si_8$, is common for typical transition-metal–metalloid glasses such as Pd–Si and Fe–B, and can be modelled with considerable success with dense random packing schemes. Chadha *et al* (1981) have found these features to be prominent in diffraction studies of nickel-based metallic glasses with boron concentrations as high as 36 at%. In fact, the difference between their data for $Ni_{82}B_{18}$ and $Ni_{64}B_{36}$ is relatively small compared with that of the rhodium-based alloys studied here. As the majority of the scattering in the diffraction experiments comes from Rh–Rh pair correlations in all cases studied here (87% for $Rh_{70}B_{22}Si_8$ as opposed to 83% for $Rh_{60}B_{32}Si_8$), it is difficult to imagine that the changes in $G(r)$ could be due to anything other than topological changes in the short-range order of the metallic glass rather than the change in weighting of the various components (whereas in $Ni_{82}B_{18}$, 93% of the scattering contribution is from Ni–Ni compared with only 83% in $Ni_{64}B_{36}$ and yet their reduced radial distribution functions are essentially the same).

The change in the short-range order of the rhodium-based metallic glasses appears from figure 2 to be a smooth and continuous one in composition rather than an abrupt transformation. The form of the distribution function for $Rh_{60}B_{32}Si_8$ is similar to some of those observed by Sinha and Duwez (1971) for Ni–Pt–P alloys, although in their case the single large maximum appears at about $R_3/R_1 \simeq 1.86$, which is unusually small. The very small peak at $R_2/R_1 \simeq 1.53$ in $Rh_{60}B_{32}Si_8$ has its counterpart in $(Ni_{20}Pt_{80})_{75}P_{25}$ as a very small maximum at $1.42\,R_1$.

The radial distribution function $4\pi r^2\rho(r)$, where $G(r) = 4\pi r(\rho(r) - \rho_0)$, gives information on the atomic coordination in the material. The average atomic density $\rho(r)$ can be written as $\rho(r) \simeq \Sigma_{ij} W_{ij}\rho_{ij}(r)$ where $W_{ij} = c_i Z_i Z_j/|\langle Z\rangle|^2$ (Cargill 1975). Here c_i is the fractional composition of constituent i, Z_i is the atomic number and $\rho_{ij}(r)$ is the atomic density of j type atoms about an average i type atom. The angular brackets denote a compositional average. For the alloys under investigation here, W_{Rh-Rh} is by far the largest of the coefficients and $W_{Rh-Rh}\rho_{Rh-Rh}(r)$ is the major contribution to the total $\rho(r)$. We therefore take the Rh–Rh coordination to be approximately

$$\eta \simeq \frac{1}{W_{Rh-Rh}} \int_0^{R_{min}} 4\pi r^2 \rho(r)\,dr$$

where R_{min} is the minimum in $\rho(r)$ following the primary maximum. These values are included in table 1 for the three alloys and exhibit, along with the nearest-neighbour distances R_1, a monotonic increase with boron concentration. Presumably this is due to the first coordination shell of rhodium atoms being pushed further away and

Table 1. Positions of the first, second, third and fourth maxima in $G(r)$ and coordination numbers and atomic densities of three rhodium-based metallic glasses.

Alloy	R_1(Å)	R_2/R_1	R_3/R_1	R_4/R_1	η	ρ(atom Å^{-3})
$Rh_{70}B_{22}Si_8$	2.74	1.51	1.67	1.95	11.48	0.08163
$Rh_{65}B_{27}Si_8$	2.77	1.49	1.65	1.94	11.52	0.08472
$Rh_{60}B_{32}Si_8$	2.80	1.53	—	1.94	11.53	0.08674

Table 2. Density, Vicker's hardness, room-temperature electrical resistivity and temperature coefficient of resistivity for three rhodium-based metallic glasses.

Alloy	ρ(g cm^{-3}) ±0.05	V_H(kg mm^{-2}) ±100	ρ_{RT}(μΩ cm) ±5	α(10^{-5} K^{-1}) ±3%
$Rh_{60}B_{32}Si_8$	9.715	1097	217.6	1.51
$Rh_{65}B_{27}Si_8$	10.136	660	185.2	3.98
$Rh_{70}B_{22}Si_8$	10.391	465	152.1	11.6

therefore increasing in size due to increasing numbers of closely coordinated boron neighbours. This also causes the width of the first coordination shell to increase as seen from the increasing full widths of the $G(r)$ from 0.57 Å to 0.60 Å to 0.61 Å for $Rh_{70}B_{22}Si_8$, $Rh_{65}B_{27}Si_8$ and $Rh_{60}B_{32}Si_8$ respectively.

The density, hardness and electrical resistivity of these alloys behave much like quite typical transition-metal–metalloid metallic glasses. From table 2, the density exhibits a predictable decrease with increasing boron concentration, although the actual atomic density (table 1) increases quite systematically. Therefore the increasing hardness may, in the simplest case, be due to the increasing rigidity of an ever denser atomic packing. The values of the Vicker's hardness are not particularly high for these alloys, considering the large metalloid content, but the trend with increasing boron concentration is typical (Ray *et al* 1977).

Table 2 also shows values for the room-temperature electrical resistivities, ρ_{RT}, and the temperature coefficients of resistivity, $\alpha = (1/\rho_{RT})(d\rho/dT)$, for the rhodium-based metallic glasses. None of the alloys were observed to be superconducting down to 1.5 K and figure 3 shows some of the low-temperature data. The increasing resistivity with increasing boron concentration is very linear and is due to the increasing disorder in the glass, as evidenced from the radial distribution functions (figure 2). The

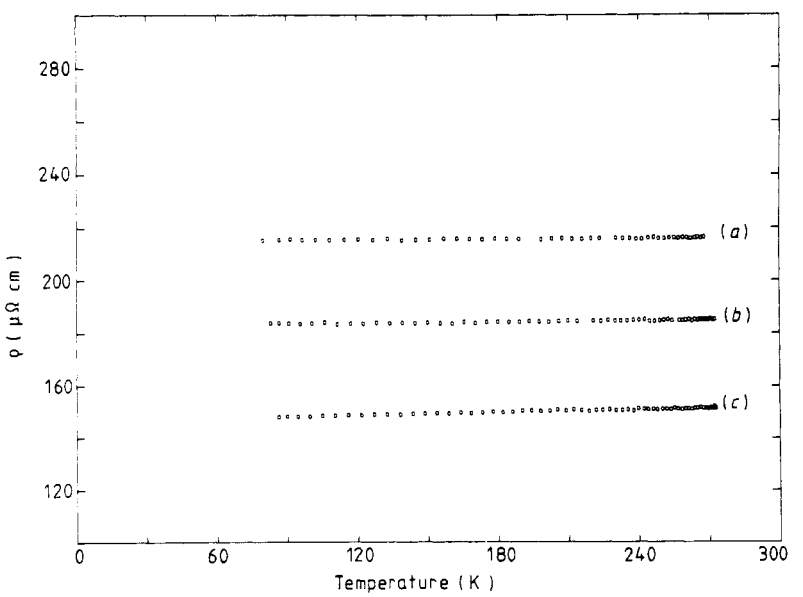

Figure 3. Low-temperature resistivity data for three rhodium-based metallic glasses. (*a*) $Rh_{60}B_{32}Si_8$; (*b*) $Rh_{65}B_2$-Si_8; (*c*) $Rh_{70}B_{22}Si_8$.

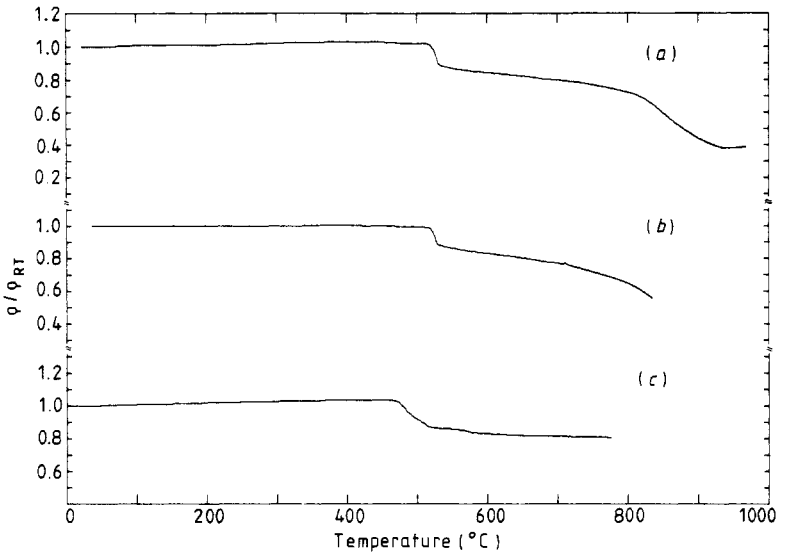

Figure 4. High-temperature resistivity data for three rhodium-based metallic glasses using a heating rate of about 12 °C min^{-1}. (*a*) $Rh_{60}B_{32}Si_8$; (*b*) $Rh_{65}B_{27}Si_8$; (*c*) $Rh_{70}B_{22}Si_8$.

temperature coefficients are considerably larger than for most disordered metallic alloys. Whereas Mooij (1973) has pointed out that very few metallic alloys with resistivities above 150 μΩ cm have a non-negative α, all three of these metallic glasses have positive temperature coefficients.

Figure 4 shows the high-temperature resistivity results, depicting crystallisation in $Rh_{60}B_{32}Si_8$ and $Rh_{65}B_{27}Si_8$ at about 525 °C. $Rh_{70}B_{22}Si_8$ crystallises at a slightly lower temperature and appears to exhibit two distinct crystallisation events. The continued negative slope of the ρ against T curve after crystallisation indicates that

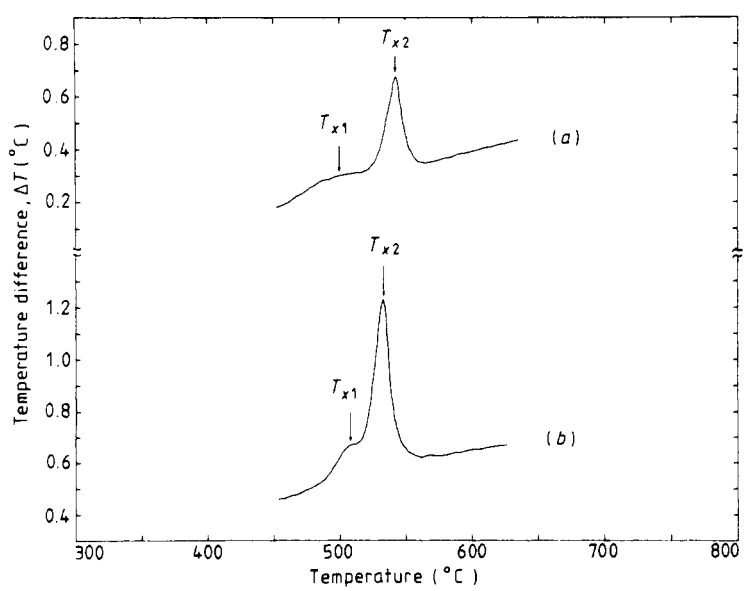

Figure 5. Differential thermal analysis data for two rhodium-based metallic glasses obtained with a heating rate of 10 °C min^{-1}. (*a*) $Rh_{60}B_{32}Si_8$; (*b*) $Rh_{70}B_{22}Si_8$.

grain growth and phase separation continue to occur for both alloys above 950 °C. This suggests that diffusion processes and crystallisation kinetics in this alloy are quite slow—a favourable condition for glass formation. The DTA studies of $Rh_{70}B_{22}Si_8$ and $Rh_{60}B_{32}Si_8$, given in figure 5, show two crystallisation events in both alloys. The high-temperature event is by far the most significant heat-generating reaction in both alloys. It is interesting to note that the metallic glass $Rh_{60}B_{32}Si_8$ is more stable than $Rh_{70}B_{22}Si_8$ with respect to crystallisation of the phase at T_{x2}, which occurs at a lower temperature for the latter glass, but less stable with respect to the phase at T_{x1}, which occurs at a higher temperature. The DTA experiments were performed for $Rh_{60}B_{32}Si_8$ at two different heating rates. At 10 °C min^{-1} the peak T_{x2} occurs at 815 K, while at 50 °C min^{-1} it occurs at 841 K. From this, an activation energy for the crystallisation can be calculated (Kirchner 1976) from

$$\Delta E = K_B \ln\left(\frac{\alpha_1 T_2^2}{\alpha_2 T_1^2}\right)\frac{T_1 T_2}{T_1 - T_2}$$

where T_1 and T_2 are peak temperatures for heating rates α_1 and α_2, respectively. For $Rh_{60}B_{32}Si_8$ the activation energy $\Delta E \simeq 80.4$ kcal mol^{-1} (or 3.48 eV per particle) which is typically within the range reported for metallic glasses (60–150 kcal mol^{-1}).

4. Conclusions

X-ray diffraction studies of $Rh_{0.92-x}B_xSi_{0.08}$ metallic glasses show a rearrangement of the short-range order as a function of composition, from a typical transition-metal–metalloid type arrangement at low boron concentrations to a much more disordered system at high concentrations. Both the x-ray data and electrical and mechanical properties suggest that the change is smooth and continuous rather than an abrupt phase transition. For all the compositions studied the behaviour of the glassy alloys is still distinctly metallic despite the presence of more than 40 at% metalloids (boron and silicon), with properties very typical of most metallic glasses. The DTA measurements show the presence of two crystallisation events with relative stabilities of the two phases changing in opposite directions as functions of composition, although the alloy comes to equilibrium very slowly, as shown by the high-temperature resistivity measurements. If there is similar competition in the glass between two types of local short-range order, presumably related to the two crystalline phases, a uniform distribution of two different orderings may be frozen in during the quenching process, the relative fractions of the two different short-range orders being composition dependent. Preliminary small-angle scattering experiments have revealed a comparatively large scattering cross section for $0.01 \leqslant K \leqslant 0.5$ Å^{-1}, which tends to support this view of a two-phase type system. The NMR data on the boron site as a function of composition may also be enlightening in determining how the symmetry of the boron site changes in going from one preferred short-range order to another as the boron concentration in the alloy is changed.

Acknowledgments

The authors would like to dedicate this paper to Professor Pol Duwez on the occasion of his seventy-fourth birthday. The continued presence, advice and good-natured

encouragement of Professor Duwez has been a constant inspiration to us all. The authors would also like to thank Mr Robert Schulz for assistance with the resistivity measurements and Angela Bressan for typing the manuscript. This work was supported by the Department of Energy under Project Agreement No DE-AT03-81ER10870 and Contract No DE-AM03-76SF00767.

References

Cargill G S III 1975 *Solid State Phys.* **30** 227 (New York: Academic)
Chadha G S, Cowlam N, Davies H A and Donald I W 1981 *J. Non-Cryst. Solids* **44** 265
Inoue A, Kitamura A and Masumoto T 1979 *Trans. Japan Inst. Met.* **20** 404
Kirchner H O K 1976 *Mater. Sci. Eng.* **23** 95
Mooij J H 1973 *Phys. Status Solidi* a **17** 521
van der Pauw L J 1958 *Philips Res. Rep.* **13** 1
Pietrokowsky P 1963 *Rev. Sci. Instrum.* **34** 445
Ray R, Hasegawa R, Chou C-P and Davis L A 1977 *Scr. Met.* **11** 973
Sinha A K and Duwez P 1971 *J. Phys. Chem. Solids* **32** 267